Journal of Network Intelligence
Taiwan Ubiquitous Information
 ISSN 2414-8105 (Online)
Volume **8**, Number **1**, February **2023**

An Optimal Filtering Algorithm for Power Equipment Monitoring System

Jin-Yang Lin, Sheng-Bin Xu, Yong-Qiang Zhang

Research Center for Microelectronics Technology
Fujian University of Technology, Fuzhou 350118, China
{7333744, 441052302, 1372148500}@qq.com

Ai-Jun Zhang*

National Engineering Research Center for Agriculture Northern Mountainous Areas
Agricultural University of Hebei, Baoding, Hebei 071000, China
xm70526@163.com

Trong-The Nguyen*

Multimedia Communications Lab.,
VNU-HCM, University of Information Technology, Vietnam
Vietnam National University, Ho Chi Minh City 700000, Vietnam
thent@uit.edu.vn

*Corresponding author: Ai-Jun Zhang, Trong-The Nguyen

Received September 14, 2022, revised October 17, 2022, accepted November 31, 2022.

Abstract. *The running power equipment states monitoring in real-time is a crucial requirement for the equipment and environment safety. This paper suggests an optimal filtering method based on a neural network with the Kalman filter optimization for a monitoring system. The hardware-based sensor acquisition and the software-based human-computer interaction interface are integrated into the proposed monitoring system. The data acquisition module transmits the collected data to the central control chip through the signal conditioning circuit and finally uploads the data to the PC for further signal filtering. A neural network with the Kalman filter optimization algorithm on the electric energy measurement is applied to increase more accuracy of current and voltage data acquisition problems. The measured data analysis of the proposed system is compared with the other algorithms in the literature. Compared results show that the suggested filtering algorithm has superior measurement accuracy, which meets the experimental requirements for a stable run system that is safe and reliable.*
Keywords: Kalman filter optimization, Electric energy metering, Filtering algorithm; Monitoring system.

1. **Introduction.** The national economy is experiencing an increase in demand for power as industry 4.0 begins to take hold [1, 2]. The smart grid technology is constantly updated and iterated [3], while the power equipment is constantly multi-functional and [4]. Whether operation of power equipment is regular, safe, and stable is related to the development of the national economy[5]. On the one hand, the monitoring technology of power equipment still retains the manual inspection monitoring part [6]. The manual inspection monitoring cannot detect power equipment in real-time and make fault warnings. The backward technical level and a large amount of manpower and material resources inevitably increase the damage rate of power equipment [7]. On the other hand, most

power equipment condition monitoring utilizes lower machine sensor data acquisition, transmission to the host computer for data processing and visual display, such as real-time equipment monitoring; early warning and analysis of equipment failure; and timely equipment maintenance [8].

However, there are some losses in the false alarms and missed opportunities of the monitoring system due to numerous unpredictable environmental elements in the detection of power equipment. Literature: A detection system based on wireless communication is used to keep an eye on electrical equipment [8, 9]. The system has a large coverage area, but in a wide range of power equipment, wireless communication is susceptible to interference from the outside world, real-time data accuracy is difficult to ensure, and energy consumption is high [10]. Based on the three-dimensional spectrum characteristics analysis method, the reference created a visual system for power equipment monitoring [10, 11]. The system first gathered and stored a lot of data, which was then characteristically examined. This method, however, has poor data refinement, high complexity, and massive amounts of calculations [12].

This paper describes the design of a power equipment monitoring system based on a neural network with the Kalman filter [12, 13] optimization using a LabVIEW. The optimal Kalman method implements the real-time voltage, current, and ambient parameter detection in the system with a neural network to process the improved data. The monitoring system can output with the equipment abnormal or raise the alarm and save historical data for each parameter to simplify inquiries. It offers superior information processing capabilities, a user-friendly upper computer interface, real-time data transfer, and high accuracy compared to conventional electric energy monitoring equipment.

2. **Power Equipment Monitoring System Design.**

This section describes the design of a power equipment monitoring system as hardware with parts, e.g., overall system design: component description, electrical energy acquisition circuit, display units, and software design.

2.1. **Overall system design.**

Figure 1 shows the power equipment monitoring system's basic structure, which is divided into two parts. One part is the lower computer part of the primary control system, composed of the main control chip, various signal acquisition sensors, LCD screens, and communication modules. The upper computer part uses LabVIEW software to design the human-computer interaction interface, which mainly includes the analysis and visualization of the lower data [13].

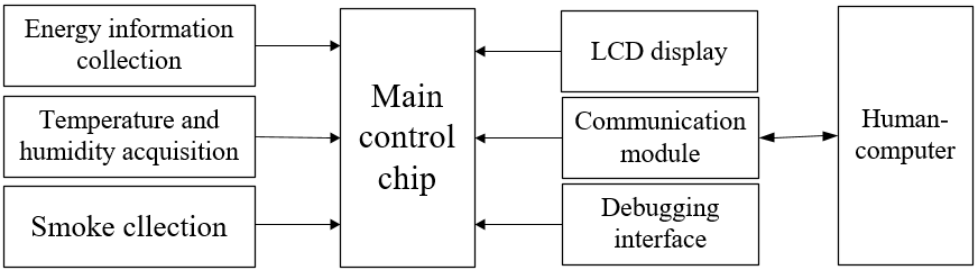

FIGURE 1. Structure of main control system

The basic principle of the power equipment monitoring system operation is as follows. The main control chip samples the electrical energy of the equipment and the surrounding environmental parameters through various external signal acquisition sensors. The signal conditioning circuit preprocess the sampled data and then transfers it to the central

control chip. The master chip parses these data to obtain all kinds of sampling values and carries out cumulative management. The voltage and current data in a period of time are obtained by filtering the power sampling values. The master chip transmits the final processed data to the communication and LCD modules. The module transmits data to the client man-machine interface. All related data are displayed to the client in the form of intuitive image charts in the human-computer interaction interface. The interface terminal has certain control functions for the main control chip to obtain the data information specified by the client. The core of the lower machine is to connect various sensors with STM32 as the main control chip, and the main control chip drives each sensor module for data acquisition and transmission [14].

2.2. **System Hardware Design.**

System components: Considering that the minimum system of a single-chip microcomputer needs to receive, process, and send many data, the Cortex-M4 core microprocessor STM32F407ZGT6, based on an ARM, is selected [15]. A high performance, rich peripheral resources, low power consumption, small size. STM32F4 has abundant peripheral interface resources, and its working frequency can reach 168Mhz. In addition, it's 32 - bit multiple AHB bus matrix gives it high access calculation speed and high and stable operating performance. It supports SWD, UART, JTAG, and three other kinds of download debugging methods. In the implementation of step-by-step debugging, only the SWCLK and SWDIO bus are connected to download and debug the code, which is the SWD download circuit. This circuit downloads fast, and the stability of program data transmission is better than the other two methods. Data transmission and reception with peripherals such as A/D chip, screen, sensor, and wireless transmission module are realized by setting different interfaces.

Electrical energy acquisition circuit design: The electric energy acquisition circuit in the system uses high-precision electric energy metering instruments to convert the required power parameter signals and filter the hardware. The measurement chip in the acquisition module selects 16-bit high-precision analog-to-digital conversion module AD7705, two data acquisition channels. The interface protocol between the A/D chip and microcontroller is the SPI protocol [16]. The parameters of the AD7705 chip are mainly set by setting the parameters of the on-chip register to debug to suit the primary control system. The interfaces with the central controller include VCC, GND, CS, SCLK, RESET, DIN, DOUT, and DRDY. The main control chip transmits data to the AD7705 chip when the DIN interface and the DOUT line access the data in the register of the metering chip. SCLK is a serial clock input that controls the transmission of data [17]. The DRDY interface is a state signal, indicating that the data's state specifies when the information is read from the register. When DRDY is low, the output register enters a new data byte. When DRDY is a high voltage, the output register data are not written to the data prompt, so the data cannot be read. CS is the chip selection interface to select the connection device.

The electric energy metering device's Structure includes the analog signal's conditioning circuit, the analog signal conversion of the A/D chip, and the interface display of the minimum system for digital signal processing and voltage and current. After controlling the digital output, the electric energy metering device uses the metering algorithm to fine-tune the digital part of the output feedback in the host computer [18].

The precision resistor and capacitor voltage divider circuit are used in voltage acquisition. The precision resistor voltage divider resolution is high, the temperature drift is s, and the capacitor is mainly de-noising[19]. A differential sampling circuit improves the attenuation signal to enhance the standard mode rejection ratio and then enters the signal

conditioning circuit [20]. The multiplier amplifies the original signal, and the subtractor reduces the signal amplitude. Finally, the optimal voltage signal input range satisfying A/D (0-5V) is obtained and input into the acquisition of the A/D conversion module [21].

High-precision current acquisition is a difficult point in electric energy measurement. Nowadays, the primary measurement methods include the shunt, fluxgate, Hall effect sensor, etc. The above three methods are compared: the shunt method is a contact measurement scheme based on Ohm's law, and the circuit current is obtained by connecting the transformer in series with the measurement circuit according to the voltage and resistance at both ends of the shunt. A four-terminal resistor is often used to design a shunt structure to eliminate measurement errors caused by lead and contact resistance. The technical principle of this method is simple, and the measurement accuracy depends on the resistance value of the divider and the measurement voltage value. The thermal effect of resistance affects the change of resistance value, which affects the accuracy of the current measurement. With the increase of current amplitude, the influence of temperature drift error is inevitable, so it is not suitable for high power current measurement. The fluxgate method is also called the DC comparator method. Usually, the standard instrument used for DC measurement calibration is called a DC comparator, and the instrument or device used for field measurement is called a fluxgate current sensor. The fluxgate method combines magnetic modulator, fluxgate, and zero flux technology to avoid power consumption and temperature drift error in traditional circuits. The disadvantage is that it is affected by the measured environmental factors and is seriously affected by electromagnetic interference in complex environments. The high price of the instrument makes the experimental cost increase exponentially. The hall effect sensor method is a non-contact measurement scheme based on the Hall effect. The potential difference of Hall element is measured, and the current is obtained according to the proportional relationship between the potential difference and the current. Its advantage is that it does not contact the measured circuit, does not consume the measured circuit power, and avoids the temperature drift error of measuring a large current. It considered factors such as experimental environment and cost [15].

Environmental parameters and display units: Environmental parameter acquisition sensors are mainly the acquisition of temperature, humidity, and smoke concentration. DHT11 is selected for temperature and moisture, which is an integrated digital sensor for humidity and temperature. The single bus communicates with the central control core, and the checksum method is used in the transmission process to ensure the accuracy of data transmission. DHT11 has low power consumption, the measurement range is 20-90 % RH, and the temperature is 0-50 °C, which meets the requirements of the experimental test. MQ-2 sensor is used to realize the function of the system monitoring smoke concentration. The working principle of the MQ-2 sensor is as follows: there is SnO_2 in the MQ-2 sensor, and the material's conductivity is small under normal conditions. However, in the case of smoke, the conductivity of SnO_2 is positively correlated with the smoke concentration. Therefore, a simple circuit containing tin dioxide can use the conductivity of tin dioxide to represent the smoke concentration. DHT11 and MQ-2 are connected to the master chip by setting the corresponding digital I/O ports. The resistance touch screen 3.5-inch TFTLCD module is selected as the display module, which has high precision, low price, strong anti-interference ability, and good stability. The display module is a four-wire resistive touch screen controller based on the XPT2046 chip. The screen is connected to PF11, PB2, PB0, PC13, and PB1 of STM32F4 by T_MOSI, T_MISO, T_SCK, T_CS, and T_PEN, [21].

2.3. **System software design.**

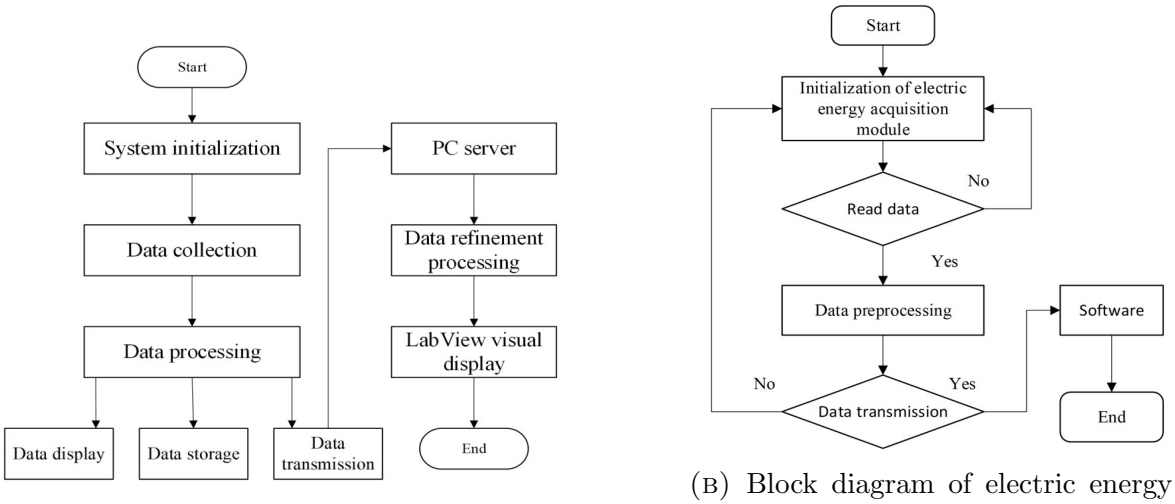

(A) System software block diagram

(B) Block diagram of electric energy information acquisition process

FIGURE 2. System design with both hardware and software

System overall software flow design: After the system is connected to the power supply, the MCU program automatically starts to run and initializes the system according to the parameters of the previous operation. The program enters the main loop. The main control unit obtains the sensor data, integrates it with the current equipment status, and sends them to the display, communication, and storage modules. The touch control on display is triggered and will automatically send the corresponding key code to the main control unit. After the corresponding keys are pressed, the main control unit obtains the signal through the input of the I/O port of the microcontroller and the timer and operates according to the corresponding instructions [16]. The data transmission is carried out by the master controller of the lower computer and the upper computer of the PC terminal through the serial communication module. The current host controller monitors that the timing function is activated. Firstly, the current RTC clock time data is obtained, and then the time data at the end of the timing is calculated according to the timing time. Each cycle determines whether the current time is equal to the timing time. When the time is similar, the timing end is judged. The system stops running and enters the standby state [17, 21].

To better realize the human-computer interaction experiment, LabVIEW is used to write the human-computer interaction module to complete the design of the human-computer interaction of the PC server [22]. The PC server software includes analyzing and using the improved algorithm to finely process terminal data and visual display in LabVIEW human-computer interaction interface. LabVIEW interface provides a serial communication function so that the PC server receives real-time data pushed by the lower computer and can also send operating instructions to the lower computer. The server software runs on the entity server with a fixed IP address to listen to whether the more inadequate computer monitoring system uploads data. If listened, it is stored in the database and processed and pushed to the display interface while providing the function of issuing instructions to modify terminal configuration parameters.

Figure 2 displays a system design with both hardware and software: a) System software block diagram and b) Block diagram of the electric energy information acquisition process.

Software design of power acquisition module: The electric energy measurement module's data mainly includes current, voltage, power, etc. The experimental power data acquisition is primarily based on a multi-channel 16 - bit ADC module. After

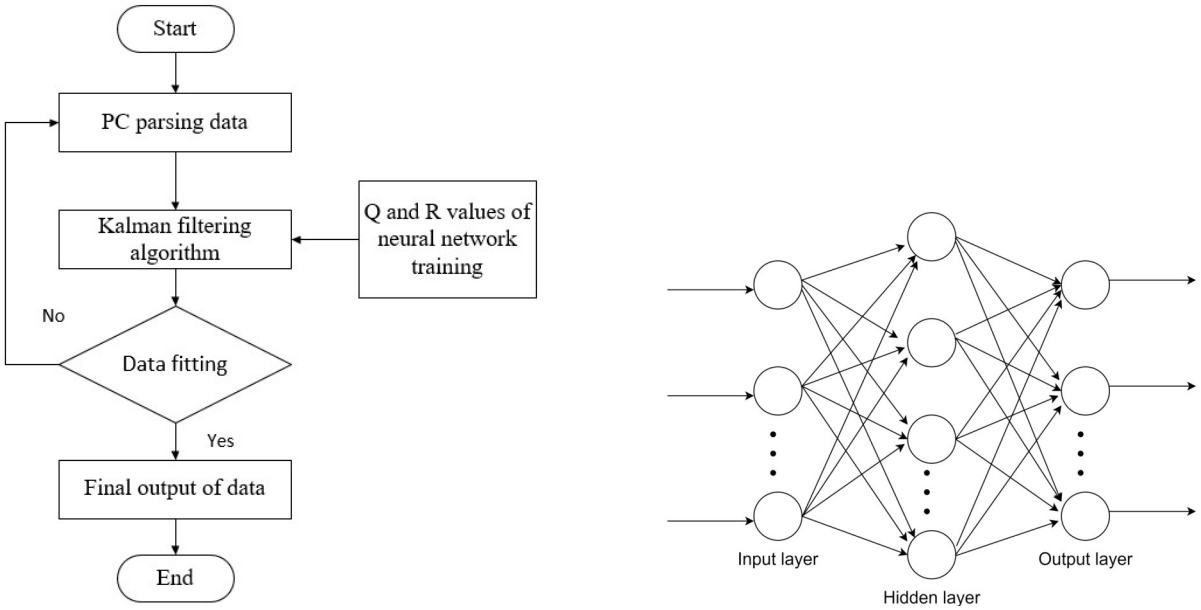

(A) Flow chart of neural network in optimizing Kalman filter

(B) A single hidden layer network structure

FIGURE 3. A flow chart of the neural network in optimizing the Kalman filter and single hidden layer network structure

the lower computer initializes the system, it is connected with the ADC chip through the SPI bus. The hardware signal processing module preprocesses the collected data. The hardware processing signal of the sampling circuit includes signal processors such as filters and amplifiers. The terminal of the power acquisition system is added with an improved software filtering algorithm for noise reduction. The lower computer transmits the preprocessed data to the upper computer for further data refinement and visualizes the sampling data with minor errors and stability. The process of the electric energy information acquisition system is shown in the figure [16, 21].

LabVIEW Visualization Module Design: The upper computer of the monitoring system in this paper is developed by LabVIEW graphical programming software. LabVIEW programming uses an intuitive graphic flow chart. This programming method is simple and easy to learn, so it has a large number of users in the field of engineering research. LabVIEW mainly includes front panel design and program block diagram design. The front panel is a visual interface when the program is running. Users can design and connect the instrument parameters through the front panel. The program block diagram is a graphical symbol that controls the controls on the front panel after creating the front panel window. The graphic compilation software has rich functions, such as recording file format, multithreading, operation control, etc. In the interface design, the principle is analyzed in depth, the design structure is refined, and the interface is designed flexibly to ensure the efficiency and stability of the power monitoring system [23].

The front panel design of LabVIEW is mainly divided into real-time data visualization and data storage. The visualization includes the configuration of communication parameters, the waveform and data display of various sensor signal monitoring, and the data storage. In this experiment, serial communication is used. The communication parameters are configured according to the corresponding parameters of the lower computer to complete the selection of the frequency and port number of the serial channel. Here, VISA serial port, index array, and other related knowledge are used.

In addition, there are also display boxes of the receiving area and sending area of the data. The monitoring interface mainly includes the collected sensor signal waveform parameters and Boolean controls to judge whether the equipment is stable or not; the collected parameters are within the specified range, the background color of the parameter control is green, and the background color of the control is red if the parameters are not within the specified range. If all parameters are within the specified range, the warning light is green, and vice versa, the light is red; through the monitoring interface, the client can intuitively observe the output signal of each sensor and whether the equipment is safe and stable. In the historical data interface, the client can view the various parameters of the monitoring system for a certain period.

There are two primary forms of view, one is the data table query, and the other is the data waveform. The historical data waveform diagram consists of the combination box control of select playback waveform and the waveform control of playback waveform. System monitoring data will be saved in the form of files on the computer for the client to view at any time [16].

Program block diagram design: step by step for system initialization, sending and receiving data, data processing, and program running termination. In the system initialization, there are local variables such as the setting of serial communication parameters, data reception and transmission, and the waveform of each parameter. The data sending and receiving part first determines whether the number of data bytes meets the requirements of the system setting. If the data transmission is displayed in the receiving area and enters the next step, otherwise the initialization is returned. The data are analyzed and classified in data processing, such as the current and voltage parameters are transformed and displayed in the waveform diagram. The Boolean indicator lights in the system that the value exceeds the set value range will alarm. After the data processing is completed, the program must end by clicking the program run termination button.

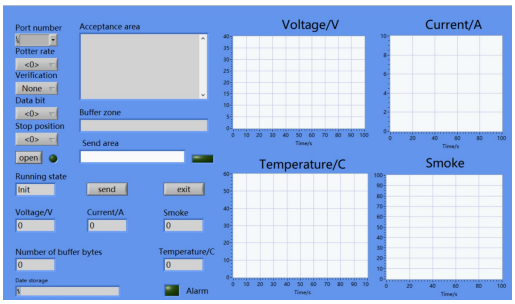

(A) Front panel design as GUI system

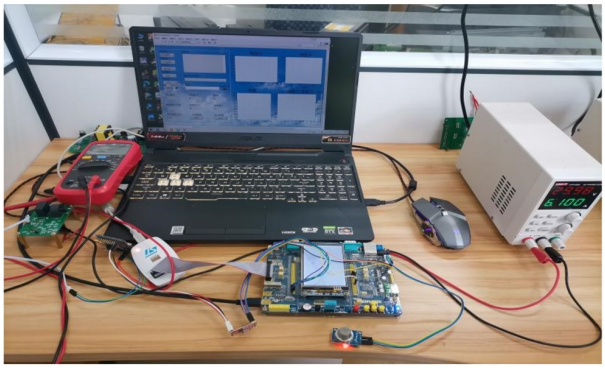

(B) Connection diagram of test equipment

FIGURE 4. The monitoring system test

3. Filtering algorithm optimization.

3.1. **Kalman filtering.** Figure 3(A) shows the flow chart of the neural network in optimizing the Kalman filter. The Kalman filter algorithm is selected as the main algorithm for software filtering. Among many filtering algorithms, the Structure of the Kalman filter algorithm is simple and easy to deploy, and it has a good combination effect with other algorithms [10]. The most important thing is that its operation is fast, which is very important for the real-time monitoring system. Here are five principal formulas for the Kalman algorithm [24].

State a priori estimation.

$$\hat{X}_{k|k-1} = F_{k-1}\hat{X}_{k-1} \tag{1}$$

Prior state estimation under the condition of prestate in step k of $\hat{X}_{k|k-1}$, posterior state estimation in step $k-1$ of $\widehat{X}_{k-1}$, F_{k-1} is drive matrix.

Error covariance update estimates can be expressed as :

$$P_{k|k-1} = F_{k-1}P_{k-1}F_{k-1}^T + Q_{k+1} \tag{2}$$

The posterior estimation covariance at time $K-1$ of P_{k-1}, and the prior estimation covariance at time $P_{k|k-1}$. Q_{k-1} process excitation noise covariance, Q is uncertain, in the calculation is not directly observed process signal.

Calculation of gain matrix:

$$K_k = P_{k|k-1}H_k^T(H_kP_{k|k-1}H_k^T + R_k)^{-1} \tag{3}$$

K_k: Kalman gain matrix, H_k: state transition matrix, R_k: measurement noise covariance is generally observable in filtering generally known conditions. The calculation K_k is used to further update the posterior state estimation at time K in real-time.

$$\hat{X}_k = \hat{X}_{k|k-1} + F_k(Z_k - H_k\hat{X}_{k|k-1}) \tag{4}$$

$\hat{X}_k$ updated posterior state estimates, Z_k measurements, and input in the filtering algorithm.

$$P_k = (I - K_kH_k)P_{k|k-1} \tag{5}$$

P_k: Error covariance matrix for step k.

3.2. **Neural network.** Figure 3(B) illustrates a single hidden layer network structure. The selection of neural network parameters can refer to the following aspects: the number of layers of the network, the number of hidden layer neurons, the number of training times, and learning efficiency [25]. In this paper, the neural network structure is selected for three layers, an input layer, a single hidden layer, and an output layer; the number of single hidden layer neurons is 11. In the following single hidden layer network structure, using three layer training network, the training network order of magnitude is moderate to avoid the problem of reducing the calculation accuracy due to the high order of magnitude. The setting of the hidden layer can be modified according to the demand, and only one layer can be used, or multiple layers can be added. The number of hidden layer neurons is also based on the request. The excessive number of nodes leads to the extension of network training time, and the training quickly falls into local optimal globality. In the experiment, every 3000 times of Kalman iterative neural network system is set to train the Kalman filter model once regularly, and the total number of training times is five. The role of learning efficiency is to constantly adjust weights, which are set to 0.03 in advance based on experience.

The neural network optimization Kalman filter algorithm [12] is used to solve the problem of large error in Kalman prediction of a nonlinear system, and the prediction ability of the optimized algorithm in the nonlinear system is effectively improved. The noise caused by the environment and hardware devices in the experimental process is real-time changed, as shown in the following figure. The host computer analyzes the data after receiving the data, and then the Kalman filter is used for data refinement. The experiment is set to train the noise values Q and R as the input parameters of the neural network after a certain number of Kalman filter iterations. The final data prediction value is the data fitting prediction value obtained by the Kalman filter value optimized by the neural network. Combined with the training results, the noise value closest to the

TABLE 1. A obtained results of voltage and current of the DC meter test

Sampling time point (s)	Standard value		Improved algorithm measurement value		Measurement Error of Improved Algorithm (%)		Kalman measurement value		Kalman measurement error (%)	
	Voltage (v)	Current (A)	Voltage (v)	Current (A)	Voltage	Current	Voltage (v)	Current (A)	Voltage	Current
5	30	6	30.106	5.983	0.35	-0.28	30.312	5.879	1.04	-2.02
10	30	5	29.883	5.019	-0.39	0.38	29.658	4.897	-1.14	-2.06
15	30	4	30.078	4.016	0.26	0.4	30.368	3.915	1.23	-2.13
20	30	3	30.085	2.985	0.28	-0.5	30.416	3.113	1.37	3.77
25	30	2.5	29.936	2.512	-0.21	0.48	29.657	2.596	-1.14	3.84
30	30	2	29.891	2.005	-0.36	0.5	29.686	1.915	-1.05	-4.25

system is determined to improve the ability of the Kalman filter to predict a nonlinear system [12, 13]. The core of this optimization algorithm is the Kalman filter algorithm. A neural network is mainly to optimize the parameters of the Kalman filter to improve the prediction accuracy and does not participate in the prediction behavior [26] .

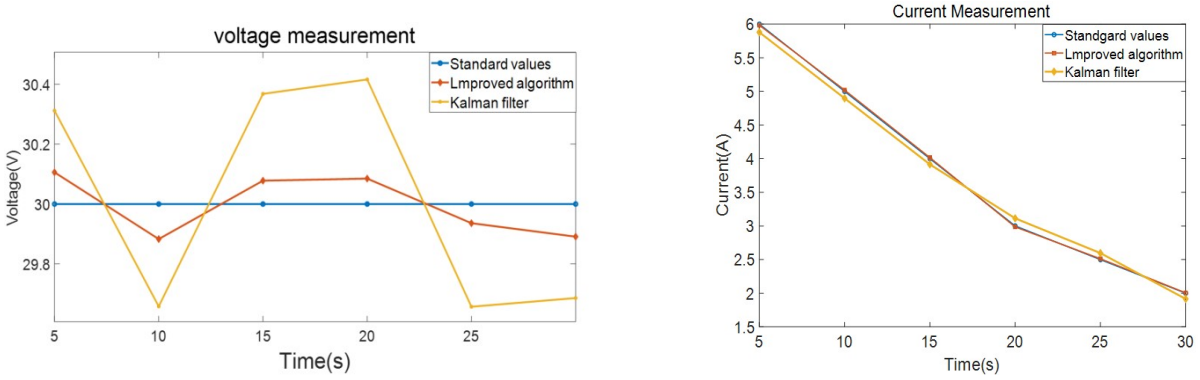

(A) Voltage measurement (B) Current measurement

FIGURE 5. A comparison of obtained data results in a line diagram of the proposed system: a) Voltage measurement and b) Current measurement

4. **Monitoring system test.**

The central controller, all kinds of sensors, power measurement modules, and a PC host computer in the lower machine are connected in the experimental test. In the experiment, the voltage and current are measured by a switching DC-regulated power supply, which outputs a maximum voltage of 32V and a maximum current of 10A. The temperature, humidity, and smoke degree are measured indoors. The experimental equipment is connected as follows. Figure 4 shows a monitoring system test: a) a GUI panel design and b) a connection diagram of test equipment.

Figure 5 shows a comparison of obtained data results in a line diagram of the proposed system: a) Voltage measurement and b) Current measurement. The data collected by each sensor of the lower computer is transmitted to the PC host computer through serial communication. The PC host computer first parses the data and then uses the improved

filtering algorithm to process the data further. Experimental data processing includes temperature and humidity, smoke concentration, voltage, and current values, and the system is set every five seconds to update the data. The measured voltage and current data are listed for comparative analysis in comparing the accuracy of filtering algorithm processing data.

Table 1 compares the voltage and recent data processing results of the suggested method with neural network optimized Kalman filtering algorithm.

Data error calculation in the experiment: the percentage of the ratio of the difference between the measured value and the typical value to the expected value. The error value of the improved algorithm in Table 1 and Figure 5 is compared with the Kalman measurement error value. It is concluded that the error value of the Kalman algorithm optimized by the neural network is smaller than that of the traditional Kalman filter algorithm, and the voltage and the current measurement value of the Kalman algorithm optimized by the neural network is closer to the standard value than that of the traditional Kalman filter algorithm.

5. **Conclusion.**

This study suggested a filtering method with a neural network in the Kalman filter optimization algorithm for a power equipment states monitoring system. The design system consists of integrated hardware and software-based human-computer interaction interface for monitoring states. The collecting data is transmitted central control chip by the data acquisition module and finally uploaded the data to the PC for further signal filtering. A Kalman filter optimization algorithm on the electric energy measurement based on a neural network is applied to increase more accuracy of current and voltage data acquisition. In the experiment, the results of detection and analysis of the system are compared with the original method, e.g., the conventional Kalman filter. Compared results show the convergence and accuracy of the proposed filtering method reduce the measurement error by less than one % and have a prominent ability to reduce noise in nonlinear time-varying systems. The test results show that the designed system has robust data analysis and real-time processing capabilities, and the system is stable and reliable as practical application value.

Acknowledgment.

This work is supported by the National Display Joint Engineering Laboratory for Flat Panel Display Technology (No. KF1802, GY-Z18038), Specific Project of Agricultural Park(Base)of Hebei Province (20536402D), Key R&D Programmers of Hebei Province (20325001D) and partially supported by the VNUHCM-University of Information Technology's Scientific Research Support Fund.

REFERENCES

[1] S. Luthra and S. K. Mangla, "Evaluating challenges to Industry 4.0 initiatives for supply chain sustainability in emerging economies," *Process Safety and Environmental Protection*, vol. 117, pp. 168–179, 2018.

[2] T-K Dao, T-T Nguyen, V-T Nguyen and T-D Nguyen, "A Hybridized Flower Pollination Algorithm and Its Application on Microgrid Operations Planning," *Applied Sciences*, vol. 12, no. 13, 6487, Jun. 2022, doi: 10.3390/app12136487.

[3] T-T Nguyen, T-G Ngo, T-K Dao and T-T-T Nguyen, "Microgrid Operations Planning Based on Improving the Flying Sparrow Search Algorithm," *Symmetry*, vol. 14, 168, Jan. 2022.

[4] C.-M. Chen, L. Chen, Y. Huang, S. Kumar, and J. M.-T. Wu, "Lightweight authentication protocol in edge-based smart grid environment," *EURASIP Journal on Wireless Communications and Networking*, vol. 2021, no. 1, p. 68, 2021.

[5] T.-Y. Wu, Y.-Q. Lee, C.-M. Chen, Y. Tian, and N. A. Al-Nabhan, "An enhanced pairing-based authentication scheme for smart grid communications," *Journal of Ambient Intelligence and Humanized Computing*, 2021, doi: 10.1007/s12652-020-02740-2.

[6] K-H Um and K- M Lee"Developing Equipment to Detect the Deterioration Status of 6.6 kV Power Cables in Operation at Power Station," *The Journal of the Institute of Internet, Broadcasting and Communication*, vol.14, no.4, pp. 179–203, 2014.

[7] Y.Wang, X.Zhai, Z.Song and Y.Geng, "A new method to detect the short circuit current in DC supply system based on the flexible Rogowski coil," *in 2011 1st International Conference on Electric Power Equipment-Switching Technology*, IEEE, 2011, pp. 237–240.

[8] A. Abu-Siada and S. Islam, "A novel online technique to detect power transformer winding faults," *IEEE Transactions on Power Delivery*, vol. 27, no. 2, pp. 849–857, 2012.

[9] M. W. Wang, Z. Yao, and H. Z. Li, " The Design of Power Equipment Monitoring System Based on Wireless Sensor Network," *in Applied Mechanics and Materials*, vol. 190, pp. 1079–1082, 2012.

[10] H. Xia, B. Li, and J. Liu, " Research on intelligent monitor for 3D power distribution of reactor core," *Annals of Nuclear Energy*, vol. 73, pp. 446–454, 2014.

[11] W. L. Chan, A. T. P. So, and L. L. Lai, " Three-dimensional thermal imaging for power equipment monitoring," *IEE Proceedings-Generation, Transmission and Distribution*, vol. 147, no. 6, pp. 355–360, 2000.

[12] S. S. Haykin and S. S. Haykin, *filtering and neural networks*, vol. 284. Wiley Online Library, 2001.

[13] Y. Wang, J. Qi, Q. Huang, L. Zhang, and X.Pan,"Design of dynamic visualization system for monitoring data of power equipment operating state," *Automation & Instrumentation*, vol. 239, pp. 59–66, 2019.

[14] X. Fan, C. Zhou, Y. Sun, J. Du, and Y. Zhao, "Research on remote meter reading scheme and IoT smart energy meter based on NB-IoT technology," *in Journal of Physics: Conference Series*, 2019, vol. 1187, no. 2, p. 22064.

[15] X. Xing, X. Huang, Y. Jin, and L. Wang," Development of a low-cost portable POCT device based on ARM," *Procedia CIRP*, vol. 70, pp. 302-306, 2018.

[16] Z. Tian et al.," Research on energy efficiency measurement scheme for electric vehicle DC charging pile," *in 2021 IEEE 4th International Conference on Electronics Technology (ICET)*, 2021, pp. 456-461.

[17] D. Gong, C. Zhang, J. Ma, C. Zhang, X. Liu, and S. Guo,"Accurate Measurement of DC Electric Energy in Power Plant," *in Journal of Physics: Conference Series*, 2022, vol. 2218, no. 1, p. 12029.

[18] T.-T. Nguyen, T.-D. Nguyen, T.-G. Ngo, and V.-T. Nguyen, "An Optimal Thresholds for Segmenting Medical Images Using Improved Swarm Algorithm," Journal of Information Hiding and Multimedia Signal Processing, vol. 13, no. 1, pp. 12-21, 2022.

[19] T.-Y. Wu, L. Wang, X. Guo, Y.-C. Chen, and S.-C. Chu, "SAKAP: SGX-Based Authentication Key Agreement Protocol in IoT-Enabled Cloud Computing, " *Sustainability*, vol. 14, no. 17. 2022, doi: 10.3390/su141711054.

[20] T.-Y. Wu, Q. Meng, S. Kumari, and P. Zhang, "Rotating behind Security: A Lightweight Authentication Protocol Based on IoT-Enabled Cloud Computing Environments," *Sensors*, vol. 22, no. 10. 2022, doi: 10.3390/s22103858.

[21] S. Sumathi, P. Surekha, and P. Surekha,*LabVIEW based advanced instrumentation systems*, vol. 728. Springer Berlin, 2007.

[22] H. A. A. Mansour, "Implementation of Chaotic Sequences on UWB Wireless Communication in Presence of NBI," *Journal of Information Hiding and Multimedia Signal Processing*, vol. 12, no. 2, pp. 82–92, 2021.

[23] J. Chao, X. Wu-bin, and L. Bing," Design of instrument control system based on LabVIEW," *TELKOMNIKA Indonesian Journal of Electrical Engineering*, vol. 11, no. 6, pp. 3427–3432, 2013.

[24] Z. GengE, H. Fang, and S. Jialun, " Design and Implementation of Cold Chain Logistics Temperature Measurement and Control System Based on LabVIEW," *in International Conference on Computer Science, Engineering and Education Applications*, 2022, pp. 194–205.

[25] W. He, N. Williard, C. Chen, and M. Pecht, " State of charge estimation for Li-ion batteries using neural network modeling and unscented Kalman filter-based error cancellation," *International Journal of Electrical Power & Energy Systems*, vol. 62, pp. 783-791, 2014.

[26] T.-T. Nguyen, T.-D. Nguyen, and V.-T. Nguyen,"An Optimizing Pulse Coupled Neural Network based on Golden Eagle Optimizer for Automatic Image Segmentation," *Journal of Information Hiding and Multimedia Signal Processing*, vol. 13, no. 3, pp. 155-164, 2022.

[27] D. Li, J. Zhou, and Y. Liu, " Recurrent-neural-network-based unscented Kalman filter for estimating and compensating the random drift of MEMS gyroscopes in real time," *Mechanical Systems and Signal Processing*, vol. 147,107057, 2021.